Supplementary material

Modeling the Influence of Chain Length on SOA Formation via Multiphase Reactions of Alkanes

Azad Madhu, Myoseon Jang, and David Deacon*
Department of Environmental Engineering Sciences, University of Florida, Gainesville, FL, USA.

KEYWORDS: Secondary organic aerosol, SOA model, Alkane SOA, Autoxidation, Photooxidation

Correspondence to: Myoseon Jang (mjang@ufl.edu)

This file includes:
5 Tables
6 Figures
References

Section S1. Autoxidation mechanism example

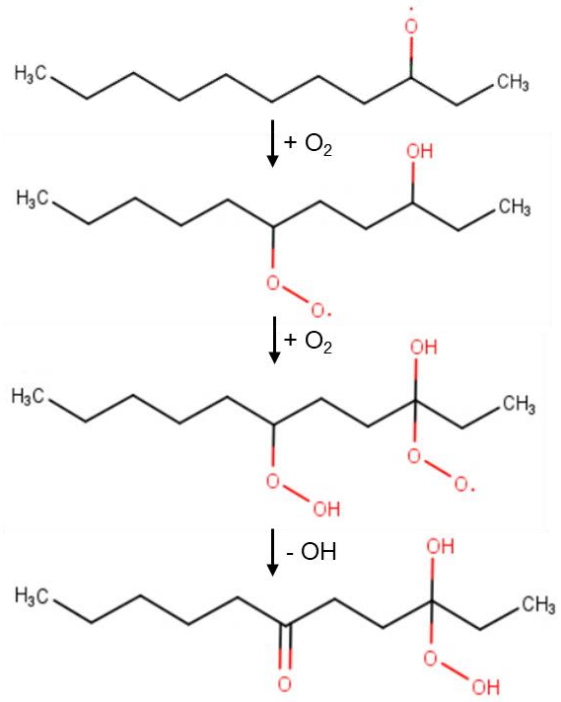

Figure S1. Example of an autoxidation reaction pathway

Section S2. Precursor wall loss rate constants

Table S1. Calculated wall loss rate constants for 4 different linear alkane precursors in the UF-APHOR chamber. A nighttime experiment was used to measure precursor wall loss to the chamber wall in the absence of photochemical oxidation. The measured data was corrected for gas dilution before wall loss rate constants were calculated. The error associated with the precursor loss rate to the wall is 2%.

Linear Alkane	Precursor loss rate constant to the wall (s^{-1})
C11	1.67D-06
C12	1.68D-06
C13	2.62D-06
C15	9.68D-06

Section S3. Prediction of product distribution using IVC

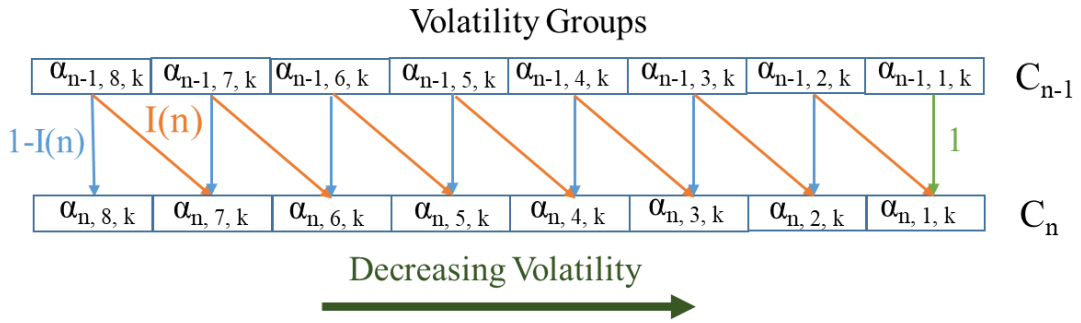

Figure S2. Construction of the product distribution of a linear alkane C_n from the product distribution of linear alkane C_{n-1} using the incremental volatility approach. This figure illustrates the process at a given reactivity level. This process must be performed for each reactivity level to construct the full product distribution array of alkane C_n. *I(n)*, the IVC, represents the portion of each α value from C_{n-1} that will be transferred to a lower volatility group in the product distribution for C_n. *1-I(n)* represents the portion of each α value from C_{n-1} that will be remain in the same volatility group in the product distribution for C_n. For the lowest volatility group, there can be no transfer to a lower volatility group so *1-I(n) = 1*.

Section S4. Parameters for the calculation of organic vapor wall loss

The mean thermal speed of the gas molecules ($\overline{v}_i$), and accommodation coefficient of *i* to the wall ($\alpha_{w,i}$) are calculated as follows:

$$\overline{v}_i = \sqrt{\frac{8Tk}{\frac{0.00314MW_i}{N_A}}} \quad \text{(S1)}$$

$$\alpha_{w,i} = e^{-0.33H_{d,i}-3H_{a,i}-0.051\alpha_i-0.61S_i-9.69} \quad \text{(S2)}$$

where $H_{d,i}$, $H_{a,i}$, S_i, and α_i represent hydrogen bond acidity, hydrogen bond basicity, dipolarity/polarizability, and polarizability of each lumping group *i*, respectively (Abraham et al., 1991; Abraham and Mcgowan, 1987; Leahy et al., 1992; Platts et al., 1999; Puzyn et al., 2010). *k* and N_A represent the Boltzmann constant and Avagadro's number, respectively.

Table S2. Parameters for the calculation of organic vapor wall loss for each lumping group

Lumping Group[a]	$H_{d,i}$	$H_{a,i}$	S_i	α_i
1MA	0.949	1.003	1.039	10.932
2MA	0.949	1.003	1.039	10.932
3MA	0.949	1.003	1.039	10.932
4MA	0.949	1.021	1.000	15.305
5MA	0.949	1.003	1.039	10.932
6MA	0.949	1.003	1.039	10.932
7MA	0.949	1.003	1.039	10.932
8MA	0.949	1.003	1.039	10.932
1P	0.521	1.581	1.518	31.647
2P	0.150	1.409	1.478	18.383
3P	0.340	1.004	1.149	18.919
4P	0.229	0.907	1.091	20.611
5P	0.250	0.831	0.991	15.295
6P	0.312	0.703	0.870	14.529
7P	0.232	0.656	0.776	13.627
8P	0.155	0.521	0.724	10.255
1S	-0.285	1.969	2.057	28.220
2S	-0.004	1.526	1.762	21.237
3S	0.084	1.304	1.516	21.253
4S	0.135	1.099	1.303	18.439
5S	0.077	1.049	1.294	17.605
6S	0.080	0.901	1.196	14.697

7S	-0.046	0.814	1.119	14.987
8S	0.058	0.707	0.931	12.848
1M	0.380	1.362	1.381	10.000
2M	0.332	1.266	1.323	10.000
3M	0.284	1.170	1.264	10.000
4M	0.532	0.973	1.132	9.704
5M	0.187	1.180	1.293	11.890
6M	0.141	0.777	0.999	16.195
7M	0.091	0.788	1.056	10.753
8M	0.043	0.689	0.956	10.013
1F	-0.253	1.501	1.747	16.168
2F	-0.253	1.409	1.677	15.062
3F	-0.253	1.317	1.607	13.955
4F	-0.253	1.225	1.537	12.848
5F	-0.253	1.075	1.376	12.848
6F	-0.253	1.057	1.415	8.475
7F	0.003	1.091	1.564	10.526
8F	0.003	0.757	1.093	8.475
1VF	0.003	1.195	1.734	30.257
2VF	0.003	1.175	1.692	27.004
3VF	0.003	1.154	1.651	23.750
4VF	0.003	1.133	1.609	20.497
5VF	0.003	1.091	1.564	18.179
6VF	-0.101	1.065	1.497	13.020
7VF	0.003	1.193	1.552	9.865
8VF	0.003	0.980	1.407	8.385

[a]MA=Multi-Alcohol, P = Partitioning only, S = Slow, M= Medium, F = Fast, VF = Very Fast. Lumping groups in red did not contain any compounds and values were extrapolated from adjacent lumping groups within the same reactivity scale.

Section S5. Reference condition for sensitivity and uncertainty

The sunlight intensity illustrated in Fig. S2 was measured on 01/20/20 in the UF-APHOR and is applied as a reference sunlight intensity for the sensitivity and uncertainty tests.

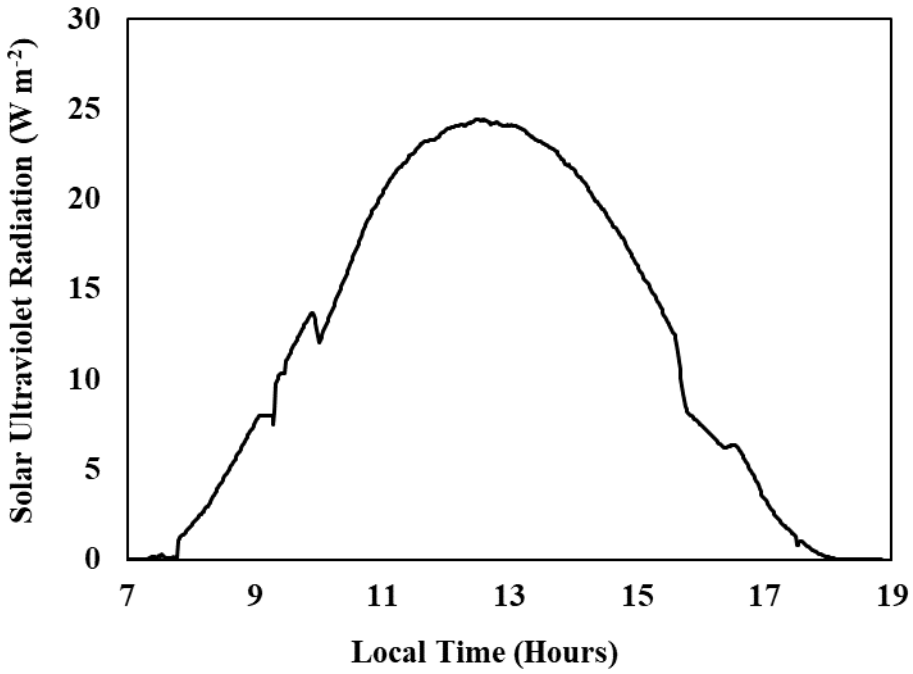

Figure S3. Local time profile of reference sunlight radiance measured by using Total Ultra-Violet Radiation (TUVR) in the UF-APHOR on 01/20/20.

Section S6. Reactions added to the CB6 Ozone gas mechanism

Table S3. Rate constants added to the CB6 ozone model for the reactions of several linear alkanes with OH. When available, rate constants were taken from the Master Chemical Mechanism (MCMv3.3.1) (Jenkin et al., 2012). Otherwise, rate constants were calculated using the structure-reactivity relationship (Kwok and Atkinson, 1995).

Linear Alkane	Reaction rate constant with OH (cm^3 $molecule^{-1}$ s^{-1})	Source
C9	2.51D-17*TEMP**2*EXP(447/TEMP)	MCM
C10	3.13D-17*TEMP**2*EXP(416/TEMP)	MCM
C11	1.29D-11	MCM
C12	1.39D-11	MCM
C13	1.6235D-11	SRR
C14	1.6763D-11	SRR
C15	1.8176D-11	SRR
C16	1.9589D-11	SRR
C17	2.1002D-11	SRR
C18	2.2415D-11	SRR
C19	2.3828D-11	SRR
C20	2.5241D-11	SRR
C21	2.6652D-11	SRR
C22	2.8067D-11	SRR
C23	2.9480D-11	SRR
C24	3.0893D-11	SRR

For chamber simulations of alkanes larger than C12 and all sensitivity and uncertainty tests, the CB6 ozone model(Cite) was used to predict precursor HC consumption, as well as concentrations of RO2 and HO2. Because CB6 is a non-explicit model, explicit reactions for several alkanes (C10, C12, C13, C15, C16, C18, C20) with hydroxyl radicals were added to predict HC consumption. For C10, and C12, available rate constants from the Master Chemical Mechanism (MCMv3.3.1) were used (Jenkin et al., 2012). For the other linear alkanes, the rate constants for each alkane with hydroxyl radicals were calculated using structure-reactivity relationship (SRR) (Kwok and Atkinson, 1995).

Section S7. Contributions of major autoxidation compounds to SOA mass

Table S4. Contributions of major autoxidation compounds to SOA mass of 4 different simulations

SOA systems	Compound(s)	% contribution to SOA Mass
C10A HC ppbC/NO_x ppb= 6.4	C103OH6OOH3NO3	61.5
	C105OH23CO5OOH	3.7
	C103OH6CO3OOH	20.9
	Total Autoxidation Products	97.5
	Total OM ($\mu g/m^3$)	352
C10B HC ppbC/NO_x ppb=2	C103OH6OOH3NO3	57.8
	C105OH23CO5OOH	5.8
	C103OH6CO3OOH	5.3
	Total Autoxidation Products	88.7
	Total OM ($\mu g/m^3$)	208
C11B HC ppbC/NO_x ppb= 22.4	C113OH6OOH3NO3	67.9
	C1123CO5OH5OOH	6.0
	C113OH6CO3OOH	18.9
	Total Autoxidation Products	92.8
	Total OM ($\mu g/m^3$)	193
C11C HC ppbC/NO_x ppb= 4	C113OH6OOH3NO3	16.0
	C1123CO5OH5OOH	1.1
	C113OH6CO3OOH	46.0
	Total Autoxidation Products	63.0
	Total OM ($\mu g/m^3$)	135
C12B HC ppbC/NO_x ppb=2.3	C123OH6OOH3NO3	41.1
	C123OH6CO3OOH	7.8
	C104OOHCO2H	23.7
	Total Autoxidation Products	73.7
	Total OM ($\mu g/m^3$)	34

C12C HC ppbC/NO_x ppb=4.9	C123OH6OOH3NO3	31.6
	C123OH6CO3OOH	16.5
	C104OOHCO2H	19.3
	Total Autoxidation Products	73.2
	Total OM ($\mu g/m^3$)	134

Section S8. Sensitivity of alkane SOA to OM_0 and acidity

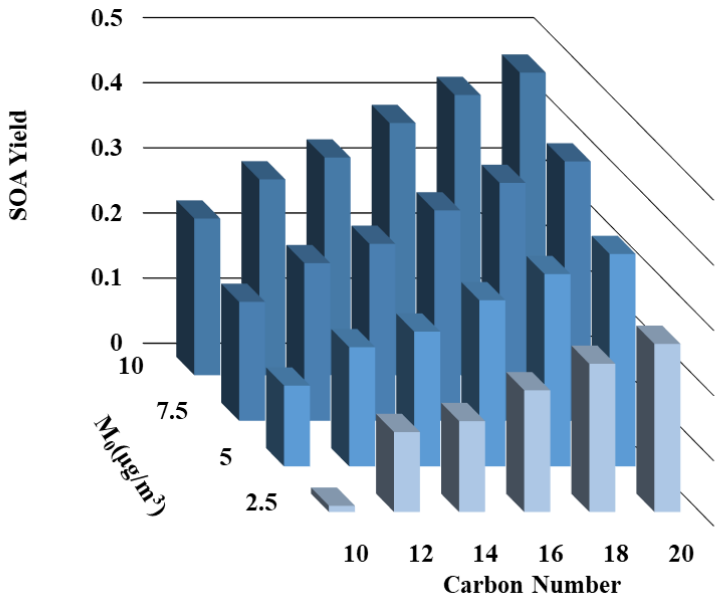

Figure S4. Simulated SOA yields for a series of linear alkanes with different values for OM_0 using the IVC-based product distributions. VOC ppbC /NO_x ppb = 3, and RH = 30%.

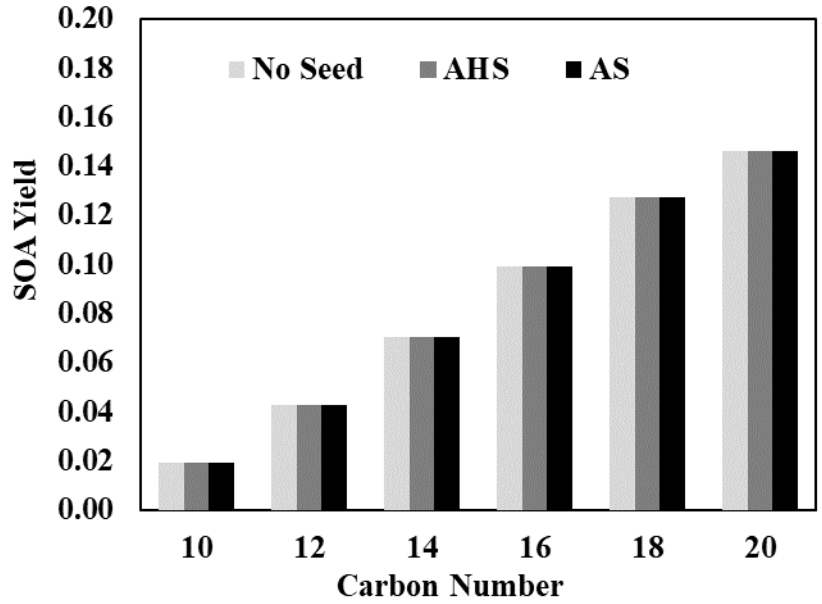

Figure S5. Simulated SOA yields for a series of linear alkanes under three different seed conditions: no seed, 10 μg/m^3 ammonium hydrogen sulfate (AHS), and 10 μg/m^3 ammonium sulfate (AS). VOC ppbC /NO_x ppb = 3, RH = 60% and OM_0 = 5 μg/m^3.

Section S9. Uncertainty due to autoxidation rate constant

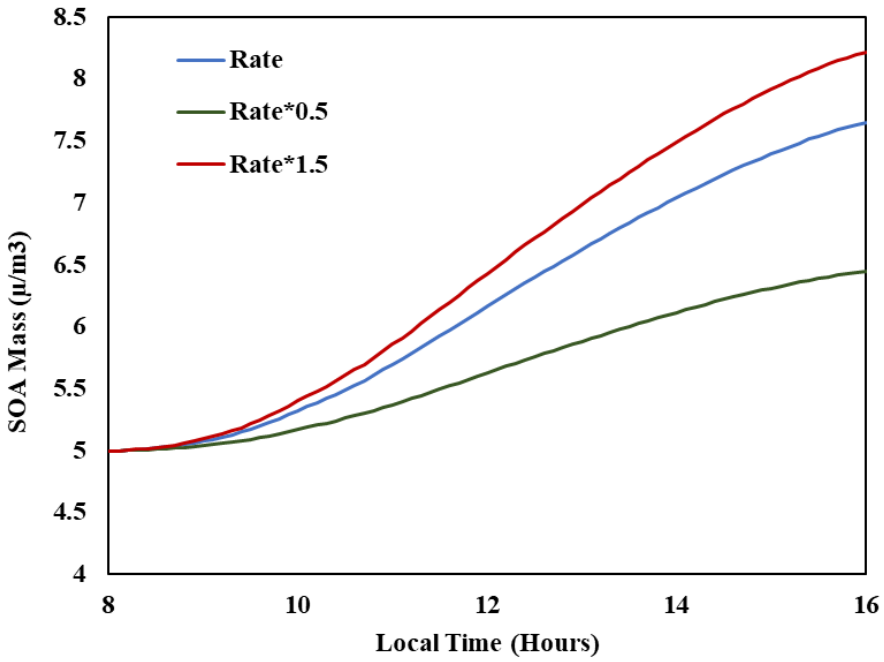

Figure S6. The impact of changing the primary rate constant responsible for the formation of autoxidation SOA mass in the C12 gas oxidation mechanism (SR1), by factors of 0.5 and 1.5, on C12 SOA formation. VOC ppbC /NO_x ppb = 3, RH = 30%, OM_0 = 5 µg/m^3, and C12 consumed = 100 µg/m^3.

Section S10. C12 autoxidation mechanism reactions and rate constants

Table S5. C12 Autoxidation reaction mechanism and rate constants

Label	Reaction	Rate Constant (cm^3 $molecule^{-1}$ s^{-1})
H-Shift Reactions [a]		
SR1	HO3C126O2 = C123OH6OOH3O2	0.8E17*EXP(-1.2077E4/TEMP) ;
SR2	C125O2 = C124OOH356CO2O2	1.2E18*EXP(-1.2077E4/TEMP) ;
SR3	C123OH6OOH3O2 = C123OH6CO3OOH + OH	1.2E17*EXP(-1.2077E4/TEMP) ;
SR4	C125OH3CO2OOH4O2 = C1223CO5OH4OOH + OH	1.2E17*EXP(-1.2077E4/TEMP) ;
SR5	NONO = C93OH6OOH3O2	1.2E18*EXP(-1.2077E4/TEMP) ;
SR6	C124OOH356CO2O2 = C123456CO2OOH + OH	1.2E18*EXP(-1.2077E4/TEMP);
SR7	C125OH3CO2OOH5O2 = C125OH23CO5OOH + OH	1.2E18*EXP(-1.2077E4/TEMP) ;
SR8	C93OH6OOH3O2 = OH + C93OH6CO3OOH	1.2E18*EXP(-1.2077E4/TEMP);
SR9	C122O2 = C125OH3CO2OOH4O2	1.2E16*EXP(-1.2077E4/TEMP) ;
SR10	C122O2 = C125OH3CO2OOH5O2	1.2E16*EXP(-1.2077E4/TEMP) ;
RO2 Autoxidation Reactions with RO2 Species [a]		
SR11	C12356CO4OOH2O2 = C122OH356CO4OOH	8.8E-13*0.2*RO2;
SR12	C12356CO4OOH2O2 = C122356CO4OOH	8.8E-13*0.2*RO2;
SR13	C12356CO4OOH2O2 = C12356CO4OOH2O	8.8E-13*0.6*RO2;
SR14	C123OH6OOH3O2 = C123OH36OOH	8.8E-13*0.5*RO2 ;
SR15	C123OH6OOH3O2 = C123OH6OOH3O	8.8E-13*0.5*RO2 ;
SR16	C125OH3CO2OOH5O2 = C1255OH3CO2OOH	8.8E-13*0.5*RO2 ;
SR17	C125OH3CO2OOH5O2 = C122OOH3CO5OH5O	8.8E-13*0.5*RO2 ;
SR18	C125OH3CO2OOH4O2 = C1245OH3CO2OOH	8.8E-13*0.2*RO2 ;
SR19	C125OH3CO2OOH4O2 = C125OH34CO2OOH	8.8E-13*0.2*RO2 ;
SR20	C125OH3CO2OOH4O2 = C125OH3CO2OOH4O	8.8E-13*0.6*RO2 ;
RO2 + HO2 Reactions [b]		
SR21	C124OOH356CO2O2 + HO2 = C12356CO24OOH	KRO2HO2;
SR22	C123OH6OOH3O2 + HO2 = C123OH36OOH	KRO2HO2 ;
SR23	C125OH3CO2OOH4O2 + HO2 = C125OH3CO24OOH	KRO2HO2 ;
SR24	C125OH3CO2OOH5O2 + HO2 = C1255OH3CO2OOH4O	KRO2HO2 ;
SR25	HO3C96O2 + HO2 = C93CO6OOH	KRO2HO2 ;
SR26	C9356CO4OOH2O2 + HO2 = C9356CO24OOH	KRO2HO2 ;
Photolysis Reactions [b]		
SR27	C923CO1CHO = CO + CO + HO2 + C6H13CO3	J(34) ;
SR28	C923CO1CHO = HCOCO + C5H13CO3	J(35) ;
SR29	C1223CO5OH4OOH = C1223CO5OH4O + OH	J(41) ;
SR30	C43CO2OOH4CHO = C412CO3O + OH	J(41) ;
SR31	C623CO1CHO = C3H7CO3 + CO + CO +HO2	J(34) ;
SR32	C623CO1CHO = C3H7CO3 + HCOCO	J(35) ;
RO2 + NO Reactions [c]		
SR33	C124OOH356CO2O2 + NO = C923CO1CHO + NO2 + CH3CHO + CO + OH	KRO2NO;

SR34	C123OH6OOH3O2 + NO = C123OH6OOH3NO3	KRO2NO*0.5;
SR35	C123OH6OOH3O2 + NO = C123OH6OOH3O + NO2	KRO2NO*0.5;
SR36	C125OH3CO2OOH4O2 + NO = C125OH3CO2OOH4O + NO2	KRO2NO ;
SR37	C125OH3CO2OOH5O2 + NO = C125OH3CO2OOH5NO3	KRO2NO*0.5;
SR38	C125OH3CO2OOH5O2 + NO = C125OH3CO2OOH5O + NO2	KRO2NO*0.5;
SR39	C9356CO4OOH2O2 + NO = C9356CO4OOH2O + NO2	KRO2NO;
Split Reactions I [b]		
SR40	C123OH6OOH3O = C104OOHCO2H + C2H5O2	2.00E14*EXP(-4714/TEMP);
SR41	C125OH3CO2OOH4O = C7H15CHO + C43CO2OOH4CHO	2.00E14*EXP(-4714/TEMP);
SR42	C125OH3CO2OOH5O = C7H15CO2H + MEKCO2	2.00E14*EXP(-4714/TEMP) ;
NO3 radical Reactions [b]		
SR43	C923CO1CHO + NO3 = C6H13CO3 + CO + CO + HNO3	KNO3AL*4.0;
SR44	C623CO1CHO + NO3 = C3H7CO3 + CO + CO + HNO3	KNO3AL*4.0 ;
Split Reactions II [b]		
SR45	C412CO3O = HCOCO + CH3CHO	KDEC ;
SR46	C12356CO4OOH2O = CH3CHO + CO + OH + C923CO1CHO	KDEC;
SR47	C1223CO5OH4O = C92OH1CHO + CH3CO3 + OH	KDEC ;
SR48	C9356CO4OOH2O = CH3CHO + CO + OH + C623CO1CHO	KDEC ;
SR49	C623CO1CHO + OH = C3H7CO3 + CO + CO + H2O	1.23E-11 ;
SR50	C923CO1CHO + OH = C6H13CO3 + CO + CO	1.23E-11;
Dimerization [a]		
SR51	C123OH6OOH3O2 = DIC123OH6OOH3OOR	1E-13*RO2 ;
SR52	C125OH3CO2OOH5O2 = DIC125OH3CO2OOH5OOR	1E-13*RO2 ;
SR53	C125OH3CO2OOH4O2 = DIC1234CO2OOH4OOR	1E-13*RO2 ;

[a]Rate constants are similar to those used by Roldin et al. (2019) [b]Rate constants used are same as rate constants for similar reactions found in MCMv3.3.1(Jenkin et al., 2012) [c]Rate constant (KRO2NO) is the same as that used for similar reactions in MCMv3.3.1.When 2 different sets of products were possible for same reactants, branching was assumed to be 50%/50%.

Compounds in Table S4 added within the autoxidation mechanism are named as follows:

1. When a compound found in MCMv3.3.1 is used, the name is left the same
2. Each compound begins with the carbon number (i.e. C12 means a 12 carbon frame)
3. Functional groups are defined by the carbon that they are attached to followed by the group (i.e. 34OH represents an OH group attached to the 3rd carbon and one attached to the 4th carbon). The order of the functional groups are as follows
    a. OH
    b. CO
    c. OOH
    d. O2, O, NO3, CO2H, CHO
        i. These functional groups are last. No conflict occurs as at most only 1 of these function are present on each compound
4. Compounds that begin with “DI” are dimer compounds

References

Abraham, M. H. and McGowan, J. C.: The Use of Characteristic Volumes to Measure Cavity Terms in Reversed Phase Liquid Chromatography, Chromatographia, 23, 243-246, 1987.

Abraham, M. H., Whiting, G. S., Doherty, R. M., and Shuely, W. J.: Hydrogen bonding: XVI. A new solute salvation parameter, π2H, from gas chromatographic data, Journal of Chromatography A, 587, 213-228, https://doi.org/10.1016/0021-9673(91)85158-C, 1991.

Jenkin, M. E., Wyche, K. P., Evans, C. J., Carr, T., Monks, P. S., Alfarra, M. R., Barley, M. H., McFiggans, G. B., Young, J. C., and Rickard, A. R.: Development and chamber evaluation of the MCM v3.2 degradation scheme for β-caryophyllene, Atmos. Chem. Phys., 12, 5275-5308, 10.5194/acp-12-5275-2012, 2012.

Kwok, E. S. C. and Atkinson, R.: Estimation of hydroxyl radical reaction rate constants for gas-phase organic compounds using a structure-reactivity relationship: An update, Atmospheric Environment, 29, 1685-1695, https://doi.org/10.1016/1352-2310(95)00069-B, 1995.

Leahy, D. E., Morris, J. J., Taylor, P. J., and Wait, A. R.: Model solvent systems for QSAR. Part 3. An LSER analysis of the 'critical quartet.' New light on hydrogen bond strength and directionality, Journal of the Chemical Society, Perkin Transactions 2, 705-722, 10.1039/p29920000705, 1992.

Platts, J. A., Butina, D., Abraham, M. H., and Hersey, A.: Estimation of Molecular Linear Free Energy Relation Descriptors Using a Group Contribution Approach, Journal of Chemical Information and Computer Sciences, 39, 835-845, 10.1021/ci980339t, 1999.

Puzyn, T., Leszczynski, J., and Cronin, M. T.: Recent advances in QSAR studies: methods and applications, 2010.